VIP | **Gas Separation** | *Very Important Paper* | Hot Paper

Molecular Trapdoor in HEU Zeolite Enables Inverse CO$_2$-C$_2$H$_2$ Separation

Jizhen Jia[+], Nana Yan[+], Xin Lian, Shanshan Liu,* Bin Yue, Yuchao Chai, Guangjun Wu, Jian Xu, and Landong Li*

Abstract: The adsorptive separation of molecules with very similar physical properties is always a challenging task. Reported herein is the design and tailoring of zeolite adsorbent for the precise discrimination and separation of CO$_2$-C$_2$H$_2$ mixture through the pronounced trapdoor effect. Typically, Sr exchanged K-type clinoptilolite, namely Sr/K-HEU, is developed as a robust zeolite adsorbent for inverse CO$_2$-C$_2$H$_2$ separation, showing the-state-of-the-art dynamic CO$_2$/C$_2$H$_2$ selectivity of 48.0 and sustainable CO$_2$ dynamic uptake of 0.96 mmol/g at the same time. The perfect recyclability and the intrinsic low-cost nature of Sr/K-HEU make it a promising candidate for practical applications. Three-dimensional electron diffraction determines the precise structure of Sr/K-HEU and density functional theory calculations reveal the intricate interplay between guest molecules and the gate-keeping extraframework cations. Briefly, extraframework Sr^{2+} cations from the ten-membered rings of HEU zeolites act as the molecular trapdoor, allowing the entry of CO$_2$ molecules while excluding C$_2$H$_2$. This work presents a new example of molecular trapdoor in zeolite and its successful application in the challenging inverse CO$_2$-C$_2$H$_2$ separation, which not only expands the scope of molecular trapdoor concept but also improves current understanding on the nature of molecular trapdoor.

[*] J. Jia,[+] Dr. S. Liu, B. Yue, Prof. Y. Chai, Prof. G. Wu, Prof. L. Li
Key Laboratory of Advanced Energy Materials Chemistry of Ministry of Education, College of Chemistry,
Nankai University,
Tianjin 300071, P.R. China
E-mail: liushanshan@nankai.edu.cn
lild@nankai.edu.cn

J. Jia,[+] Dr. X. Lian, Dr. S. Liu, B. Yue, Prof. J. Xu
School of Materials Science and Engineering,
Nankai University,
Tianjin 300350, P.R. China

Dr. N. Yan[+]
National Engineering Research Center of Lower-Carbon Catalysis Technology, Dalian Institute of Chemical Physics, Chinese Academy of Sciences,
Dalian 116023, P.R. China

Prof. L. Li
Frontiers Science Center for New Organic Matter,
Nankai University,
Tianjin 300071, P.R. China

[+] Jizhen Jia and Nana Yan contributed equally to this work.

Introduction

Acetylene (C$_2$H$_2$) stands as an important industrial raw material, serving not merely as vital gas fuel, but more importantly as a key feedstock for the production of valuable chemicals and synthetic materials.[1–3] C$_2$H$_2$ can be obtained from the partial combustion of natural gas and the steam cracking of hydrocarbons, with the co-production of a significant amount of carbon dioxide (CO$_2$).[4,5] Consequently, the separation of CO$_2$ from C$_2$H$_2$ to secure high-purity C$_2$H$_2$ is an essential step for its downstream applications. Liquid extraction and cryogenic distillation are currently employed as the predominant technologies in industry to obtain high-purity C$_2$H$_2$ from the mixtures containing CO$_2$ and C$_2$H$_2$, which unfortunately suffer from substantial drawbacks such as huge energy consumption, high operating cost, and environmental unfriendliness.[6,7] A surge of interest has arisen in the quest for more sustainable and cost-effective CO$_2$-C$_2$H$_2$ separation technologies. Thereinto, the adsorptive separation emerges as a promising alternative, relying on the availability of adsorbents with high dynamic uptake and selectivity.[8–10] The formidable challenges in the adsorptive separation of CO$_2$-C$_2$H$_2$ are obvious due to the molecular resemblance shared by CO$_2$ and C$_2$H$_2$, for example the kinetic diameter and physical properties including the boiling point, the dipole moment as well as the polarizability (Supporting Information, Table S1).[6,7,11]

Various porous adsorbents have been explored for CO$_2$-C$_2$H$_2$ separation, and most of them preferentially trap C$_2$H$_2$ with moderate selectivity, owing to the slightly higher polarizability and quadrupole moment of C$_2$H$_2$.[12–18] This necessitates further desorption processes to attain high-purity C$_2$H$_2$, thereby engendering a convoluted separation process and exacerbating energy wastage. In contrast, the allure of CO$_2$-selective adsorbents lies in their ability to facilitate the direct acquisition of high-purity C$_2$H$_2$ in a single step. However, the development of such CO$_2$-selective adsorbents is a very challenging task, and only a handful of metal-organic frameworks (MOFs) have been reported so far.[19–25] The regulation of adsorption sites,[26,27] control of pore environment,[28–31] and kinetic-sieving[21,32,33] have been proposed as available features to optimize CO$_2$ recognition by MOFs for inverse CO$_2$-C$_2$H$_2$ separation.

Zeolites have been widely used as industrial adsorbents for decades, showing unparalleled advantages of good stability, large-scale availability and low production cost.[34–36] Adsorptive separation by zeolites is mainly based

on physisorption and size-sieving, usually not applicable for the challenging CO_2-C_2H_2 separation. In fact, the efficient CO_2-C_2H_2 separation has only been achieved with Cu@FAU zeolite wherein C_2H_2 molecules are selectively trapped through reversible chemical bonding on coordinatively unsaturated Cu sites confined in zeolite.[37] It seems very difficult to obtain a CO_2-selective zeolite adsorbent for efficient CO_2-C_2H_2 separation considering the fact that the ubiquitous local electrostatic field within zeolites will exhibit stronger affinity toward C_2H_2 molecules with higher polarizability and larger quadrupole moment than CO_2. On the other hand, the adsorption behaviors of guest molecules on zeolites show great diversity, among which an interesting mechanism, namely the trapdoor effect, a subset of the so-called gating flexibility, has been disclosed.[38–41] Typically, the accessibility of the guest molecules to the internal cavities is determined by their ability of inducing temporary and reversible cation deviation to open the door for entering.[42] This mechanism usually occurs in small-pore zeolites with eight-membered rings (8MRs) windows and large gate-keeping cations (K$^+$ and Cs$^+$), by which efficient CO_2-CH_4 and CH_4-N_2 separations have been achieved.[43–45] The trapdoor effect by zeolites may offer new opportunities for the challenging inverse CO_2-C_2H_2 separation.

Herein, the trapdoor effect by Sr-exchanged K-type clinoptilolite (Sr/K-HEU) zeolite is disclosed for the first time and successfully applied in the inverse CO_2-C_2H_2 separation. Typically, the state-of-the-art CO_2/C_2H_2 dynamic selectivity of 48.0 with high CO_2 dynamic uptake of 0.96 mmol/g can be achieved in the separation of CO_2-C_2H_2->He mixture (5/10/85; v/v/v) under optimized conditions. The fine structure of Sr/K-HEU with the precise positioning of extraframework cations is identified by means of three-dimensional electron diffraction (3D ED). The interaction between guest molecules (CO_2 and C_2H_2) and gate-keeping cations (K$^+$ and Sr^{2+}) is investigated by theoretical simulations, showing a full picture of molecular trapdoor in inverse CO_2-C_2H_2 separation by Sr/K-HEU zeolite. This study not only provides a new example of trapdoor effect in zeolites for a challenging adsorptive separation process, but also improves our understanding on the underlying mechanism of molecular trapdoor.

Results and Discussion

HEU zeolite boasts a distinctive two-dimensional (2D) microporous channel system, characterized by two parallel channels comprised of 10-membered rings (channel A) and 8-membered rings (channel B), intersected by additional 8-membered rings (channel C), ultimately culminating in a layered architectural configuration.[46] Commercial K-HEU zeolite (Si/Al = 3.9) exhibits considerable adsorption capacities for both CO_2 and C_2H_2 (2.48 and 2.05 mmol/g for CO_2 and C_2H_2, respectively, Figure 1a). The microporous surface area of K-HEU calculated from Ar adsorption-desorption isotherms at 87 K is close to zero, demonstrating that Ar molecules cannot diffuse into the pores of zeolite (Supporting Information, Figure S1, Table S2). The great difference
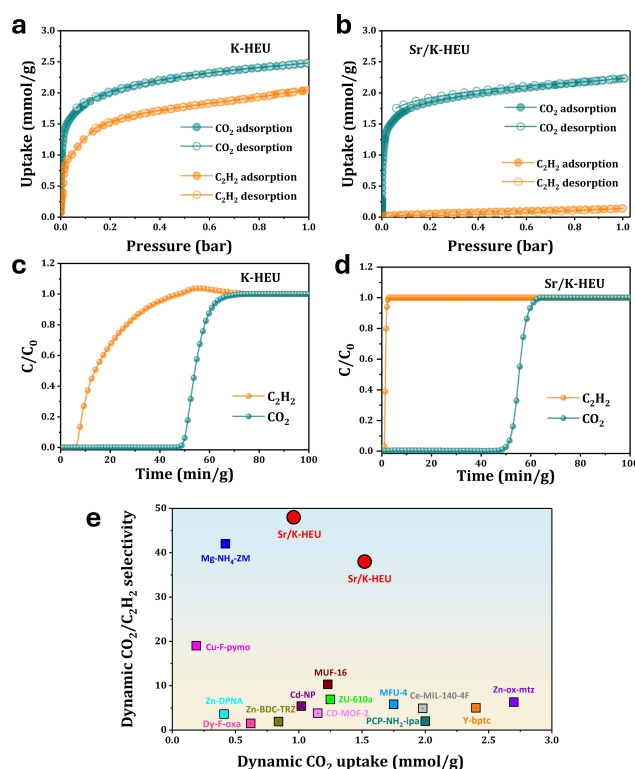

Figure 1. Adsorption isotherms of C_2H_2 and CO_2 on K-HEU (**a**) and Sr/K-HEU (**b**) at 298 K; Column breakthrough curves of CO_2/C_2H_2/He (5/10/85, v/v/v; total gas flow: 8.5 mL/min) over a fixed-bed reactor packed with K-HEU (**c**) and Sr/K-HEU (**d**) at 298 K; (**e**) Plots of CO_2/C_2H_2 dynamic selectivity against dynamic CO_2 uptake under ambient conditions with representative adsorbents.

in the sorption performance of K-HEU zeolite toward molecules with similar kinetic diameters (3.4 Å for Ar and 3.3 Å for CO_2) implies that K-HEU might selectively open the door for CO_2 molecules, following the so-called trapdoor effect.[44,45] Unfortunately, K-HEU exhibits molecular trapdoor effect for both C_2H_2 and CO_2, resulting in poor separation ability. It is known that the interaction between extraframework cations and gas molecules plays a pivotal role in the observed molecular trapdoor effect, and thereby, it should be possible to achieve specific recognition of CO_2 *via* molecular trapdoor effect for CO_2-C_2H_2 separation simply by regulating the extraframework cations.

A series of alkaline-earth metal ion-exchanged M-HEU [M = Mg(II), Sr(II), Ba(II), with residual K(I)] zeolites were prepared for CO_2-C_2H_2 adsorption and separation {due to the severe collapse of Ca/K-HEU framework during calcination process (Supporting Information, Figure S2, S9 and S10)[47–49], it is not included in this study}. The XRD patterns, SEM images and Ar sorption isotherms of obtained zeolite samples are shown in Figure S1, S3–S4 (Supporting Information). Typically, M-HEU zeolites exhibit similar Ar sorption characteristics as K-HEU, and therefore, their microporous properties were determined by CO_2 sorption isotherms at 196 K (Supporting Information, Table S2). M-HEU zeolites achieve high exchange degrees of >80% after three consecutive ion-exchange processes (Supporting Informa-

tion, Table S2), consistent with previous reports.[50] The CO_2 and C_2H_2 sorption isotherms of M-HEU zeolites were measured at 298 K and 1 bar (Figure 1a–b, Supporting Information, Figure S5–S6). The saturated CO_2 adsorption capacities of M-HEU zeolites align closely with their micropore surface areas (Supporting Information, Figure S1, Table S2). In this context, regulating the extraframework cations of HEU zeolites to exclude C_2H_2 molecules becomes a feasible strategy to achieve one-step CO_2-C_2H_2 separation. As expected, the adsorption capacities of C_2H_2 display significant variations across various cations (Ba/K-HEU > K-HEU > Mg/K-HEU ≫ Sr/K-HEU), indicating a close correlation between the ability of C_2H_2 molecules to penetrate the structure and the presence of gate-keeping extraframework cations. Remarkably, Sr/K-HEU maintains a substantial uptake of CO_2 (2.21 mmol/g) while demonstrating only minimal uptake of C_2H_2 (0.14 mmol/g) at 298 K and 1 bar. Sr/K-HEU exhibits a noteworthy CO_2/C_2H_2 saturated uptake ratio of 15.8, surpassing that of known CO_2-selective adsorbents such as Cu-F-pymo (11.9),[26] MUF-16 (11.9 at 293 K),[28] Cd-NP (6.02),[29] Mg-NH$_4$-ZM (6.2),[30] Zn-ox-mtz (12.8),[31] and Ce^{IV}-MIL-140-4F (2.7)[32] (Supporting Information, Table S3). It underscores the potential of Sr/K-HEU zeolite as a low-cost adsorbent for CO_2-C_2H_2 separation due to the gate-keeping function of Sr^{2+}, which selectively permits the passage of CO_2 molecules while hindering that of C_2H_2 (*vide infra*).

To assess the practical viability of M-HEU for CO_2-C_2H_2 separation, column breakthrough experiments for CO_2/C_2H_2/He mixture (5/10/85; v/v/v) were conducted at 298 K (Figure 1c–d, Supporting Information, Figure S7–S8). In consistent with static uptake results, all M-HEU zeolites exhibit earlier breakthrough of C_2H_2 than CO_2, and almost pure C_2H_2 (determined by the mass spectrum detection limit of 1 ppm) can be obtained prior to the breakthrough of CO_2, for example 45 min for Sr/K-HEU. The dynamic adsorption capacities of CO_2 for K-HEU, Mg/K-HEU, Sr/K-HEU and Ba/K-HEU are measured as 0.95, 0.66, 0.96 and 0.88 mmol/g, respectively. Accordingly, the dynamic separation selectivity of CO_2/C_2H_2 is determined as 3.1, 4.9, 48.0 and 2.5, respectively. Remarkably, the dynamic selectivity of Sr/K-HEU surpasses all known CO_2-selective adsorbents, including prominent MOFs, for instance, Cu-F-pymo (19.0),[26] MUF-16 (10.3),[28] Cd-NP (5.4),[29] Mg-NH$_4$-ZM (42.0),[30] Ce^{IV}-MIL-140-4F (4.9)[32] and Y-bptc (33.0)[23] (Supporting Information, Table S3). A comparison of experimentally-determined CO_2/C_2H_2 dynamic selectivity against dynamic CO_2 uptake further underscores the unprecedent performance of Sr/K-HEU in CO_2-C_2H_2 separation (Figure 1e). Sr/K-HEU appears to be the most selective adsorbent for inverse CO_2-C_2H_2 separation with sustainable CO_2 dynamic uptake. To our knowledge, Sr/K-HEU is the first eligible zeolite adsorbent for inverse CO_2-C_2H_2 separation. The impacts of operating conditions on CO_2-C_2H_2 separation on Sr/K-HEU were further investigated. The dynamic CO_2 uptake and CO_2/C_2H_2 selectivity keeps nearly unchanged with increasing gas flow rate from 8.5 to 20 mL/min, and the dynamic CO_2 uptake only shows a slight decrease with increasing temperature from 298 to 333 K

(Supporting Information, Figure S11–S15). Especially, the dynamic CO_2 uptake at 298 K increases to 1.52 mmol/g while the dynamic C_2H_2 uptake keeps unchanged at 0.04 mmol/g in high-concentration CO_2-C_2H_2 mixture (50/50; v/v) (Supporting Information, Figure S16). These results demonstrate the feasibility of Sr/K-HEU zeolite adsorbent for practical applications.

Temperature-programmed desorption (TPD) experiments were conducted to assess the adsorption strength and the recyclability of adsorbents. In a typical procedure, the zeolite adsorbent underwent initial dosing with a gas mixture of CO_2-C_2H_2 at 298 K, followed by primary Ar purging at the same temperature. Subsequently, TPD profiles of C_2H_2 and CO_2 were recorded in the temperature range of 298 to 650 K under flowing Ar. In principle, weakly adsorbed C_2H_2 and CO_2 molecules on adsorbents can be swiftly removed during the primary purging process, while the strongly adsorbed species are trapped in the adsorbents. As shown in Figure 2a, very weak C_2H_2 desorption peaks can be observed in the C_2H_2-TPD profile of Sr/K-HEU, indicating that trace weakly adsorbed C_2H_2 molecules on Sr/K-HEU are eliminated during the primary purging process. In contrast, distinct multiple C_2H_2 desorption peaks are observed in the temperature range of 323–500 K for Mg/K-HEU, Ba/K-HEU and K-HEU, in consistency with the results from static adsorption and dynamic breakthrough experiments. On the other hand, all M-HEU zeolites show
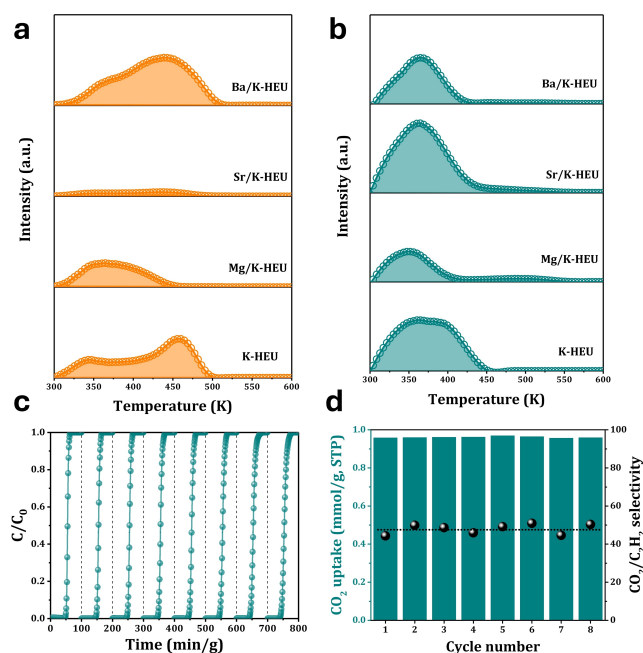
Figure 2. TPD profiles of (**a**) C_2H_2 and (**b**) CO_2 on M-HEU zeolites after saturated adsorption. Recycling performance of Sr/K-HEU at 298 K and 1 bar with a gas mixture of CO_2/C_2H_2/He (5/10/85, v/v/v) and total flow rate of 8.5 mL/min: (**c**) Recyclability of Sr/K-HEU in C_2H_2/CO_2 separation for eight cycles (only the CO_2 concentration curves are shown for conciseness); (**d**) Dynamic adsorption capacities of CO_2 and dynamic selectivity of CO_2/C_2H_2 in eight cycles. The saturated adsorbent was regenerated by heating at 473 K in flowing Ar for 30 minutes to remove adsorbed CO_2 between cycles.

Forschungsartikel

Angewandte
Chemie

distinct CO_2 desorption peaks in the temperature range of 298–453 K and Sr/K-HEU shows the largest CO_2 desorption peak among all samples under study (Figure 2b). According to the TPD profiles, the complete regeneration of M-HEU adsorbents can be achieved upon thermal treatment at 453 K or higher. As expected, the optimized Sr/K-HEU adsorbent shows perfect recyclability in eight continuous cycles of binary breakthrough experiments (Figure 2c). The dynamic CO_2 uptake (average: 0.96 mmol/g) and the CO_2-C_2H_2 selectivity (average: 47.8) can be well maintained in the recycling breakthrough tests (Figure 2d). These results highlight the straightforward temperature-swing adsorption process for CO_2-C_2H_2 separation employing Sr/K-HEU as a low-cost zeolite adsorbent (~\$2000 per ton).

To validate the adsorption affinity between CO_2 and M-HEU, the isosteric heats of adsorption (Q_{st}) of CO_2 within these zeolites were determined *via* TG-DSC measurements (Supporting Information, Figure S17–S20). The Q_{st} values obtained for M-HEU are 23.9, 28.2, 29.3 and 30.0 kJ/mol for Mg/K-HEU, Sr/K-HEU, K-HEU and Ba/K-HEU, respectively. All M-HEU zeolites exhibit desirable adsorption heat values of 30 kJ/mol at most, indicating the nature of physisorption. For the optimized adsorbent Sr/K-HEU, the isosteric heat was also calculated using the Clausius-Clapeyron equation from the isotherms measured across a range of temperatures (Supporting Information, Figure S21). The isosteric heat value of ~30 kJ/mol can be obtained (Supporting Information, Figure S22), in consistency with

that measured by TG-DSC. The data of isosteric heat further validate the good recyclability of Sr/K-HEU for CO_2-C_2H_2 separation.

Upon scrutiny of the empirical findings delineated above, it is rational to propose that the inverse CO_2-C_2H_2 separation is achieved by the trapdoor effect of extraframework cations in M-HEU zeolites, with delicate interplay between the guest molecules and the gate-keeping cations. The underlying mechanism in the molecular level is then explored, starting from the precise identification of extraframework cations in HEU zeolite. 3D ED technique was performed to unveil the crystallographic structure of Sr/K-HEU ($|Sr_{10}K_2|[Al_{22}Si_{86}O_{216}]$) and the location of extraframework cations. The high-quality 3D ED data (resolution 0.8 Å) was collected within 3 min (Supporting Information, Table S4). The possible space group (*C2*, *Cm*, and *C2/m*) can be deduced from reflection conditions of the reconstructed 3D reciprocal lattice (Supporting Information, Figure S23). The initial structure of Sr/K-HEU was solved by SHELXT[51] with the space group of *C2/m* and unit cell parameters of a = 17.0 Å, b = 17.4 Å, c = 7.4 Å, α = 90°, β = 113.9°, and γ = 90°. The locations of extraframework cations were identified by subsequent refinement *via* SHELXL.[51] Conclusively, the architectural framework of Sr/K-HEU contains a 2D channel system, wherein 10MRs and 8MRs course along the [001] axis, denoted as channels A and B, respectively (Figure 3a). Channel C comprises 8MRs aligned along [100] (Figure 3d), and it is dense without pores along
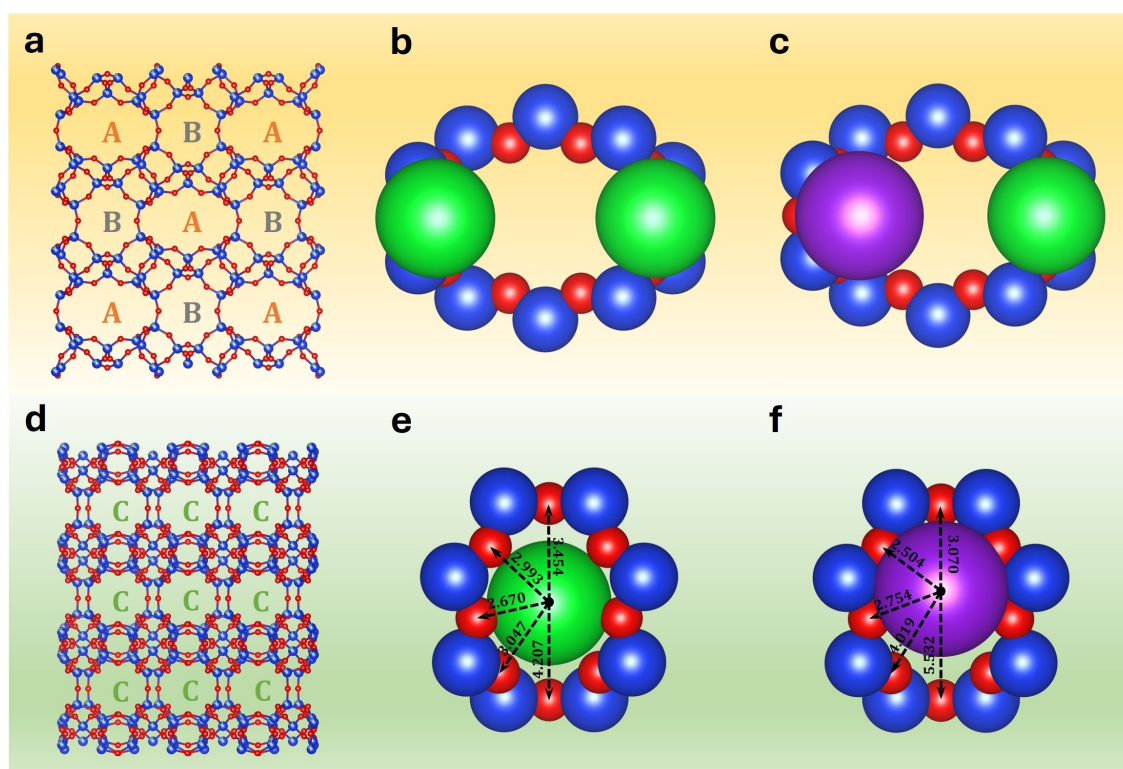

Figure 3. Views of framework structure and cation sites of Sr/K-HEU determined from 3D ED. The 10MRs and 8MRs run along [001] as channel A and channel B, respectively (**a**), and the 8MRs run along [100] as channel C (**d**). The extra-framework cations are located in the 10MR of channel A as 10MR-Sr/Sr (**b**) and 10MR-K/Sr (**c**), while occupying channel C as Sr^{2+} (**e**) and K^+ (**f**). Si/Al: blue; O: red: Sr: green; K: purple.

the [010] direction, a configuration consistent with previous reports.[52–54] Extra-framework cations, including Sr^{2+} and un-exchanged residual K^+, stake their claim within 10MRs of channel A (Figure 3b-c) and also pervade 8MRs of channel C coordinating with framework oxygen atoms (closest Sr–O distance: 2.670 Å, closest K–O distance: 2.504 Å) (Figure 3e-f). It should be noted that, in consistent with the proportional distribution of cations, the 10MRs within channel A may be settled by double Sr^{2+} cations (Figure 3b) or Sr^{2+}-K^+ pairs (Supporting Information, Figure S24, Figure 3c).

In light of the complete blockage of the 8MRs within the channel C of Sr/K-HEU (Figure 3e-f), the possibility of molecules adsorption in the channel C can be fully ruled out. By analyzing the apparent difference between the properties of Ba/K-HEU and Sr/K-HEU, it can be concluded that the adsorption difference should not originate from the similar parts of the two zeolites (fully exposed 8MRs), but should come from the different parts, namely the 10MRs sheltered by different cations. The density distribution results also indicate that under the premise of guest molecule (CO_2 and C_2H_2) admission into internal cavities (Supporting Information, Figure S25), the molecules are only distributed along the channel A, so it is established from theoretical calculations that the 10MRs of channel A represent the sole pragmatic conduits for gas diffusion into the internal cavities. This revelation prompts an inquiry into the mechanism for the admission of guest molecules despite the apparent occlusion of the pore entrance in Sr/K-HEU. The only possibility is the robust interaction between guest molecules and the gate-keeping cations, which triggers a transient and reversible cation deviation, thus facilitating the entry of specific guest molecules into the internal cavities through the door of 10MRs. That is, the concept denoted as the "trapdoor" effect in previous reports.[44,45,55] To unravel

the complexity of the guest admission process by the 10MRs of Sr/K-HEU, DFT calculations were performed to demonstrate the relative energy level for guest molecules to navigate past the gate-keeping cations. The initial state energy of the guest molecules prior to their approach to the 10MRs is set at 0 kJ/mol. The consequential energy differential, denoted as ΔE, represents the augmentation in energy level with the presence of guest molecules relative to the initial state energy. The snapshots capturing the adsorption configurations and trajectories of guest molecules and gate-keeping cations within the confined space of the 10MRs of Sr/K-HEU were investigated in detail. Both K^+ and Sr^{2+} are considered as the gate-keeping cations considering their co-presence in Sr/K-HEU (17 % K^+ and 83 % Sr^{2+}). The calculation model is based on the 3D ED resolved structure and the ratio of K^+/Sr^{2+}.

The interaction between CO_2 and K^+ from the 10MRs settled by Sr^{2+}-K^+ pairs (denoted as 10MR-K/Sr) was studied first. Typically, the interaction between CO_2 and K^+ initiates first a pivotal repositioning of the latter towards the center of the ring, effectuating complete occlusion (a transitional state mandating an energy barrier of 57 kJ/mol), then towards the periphery of the ring, transiently unblocking door of the 10MRs (a migration state necessitating an energy barrier of 36 kJ/mol), facilitating unimpeded passage of CO_2. Subsequently, as CO_2 traverses further into the internal cavities, K^+ promptly reverts to its initial position to lock the door, thereby attaining the energy nadir of the system (Figure 4a). For the interaction between CO_2 and Sr^{2+} from the 10MRs settled by Sr^{2+}-K^+ pairs, similar dynamics could be observed. Briefly, the interaction between CO_2 and Sr^{2+} first initiates a subtle shift of Sr^{2+} towards the center of the ring (a transition state demanding an energy barrier of 44 kJ/mol), followed by a deviation towards the periphery to unblock the door of 10MRs (with
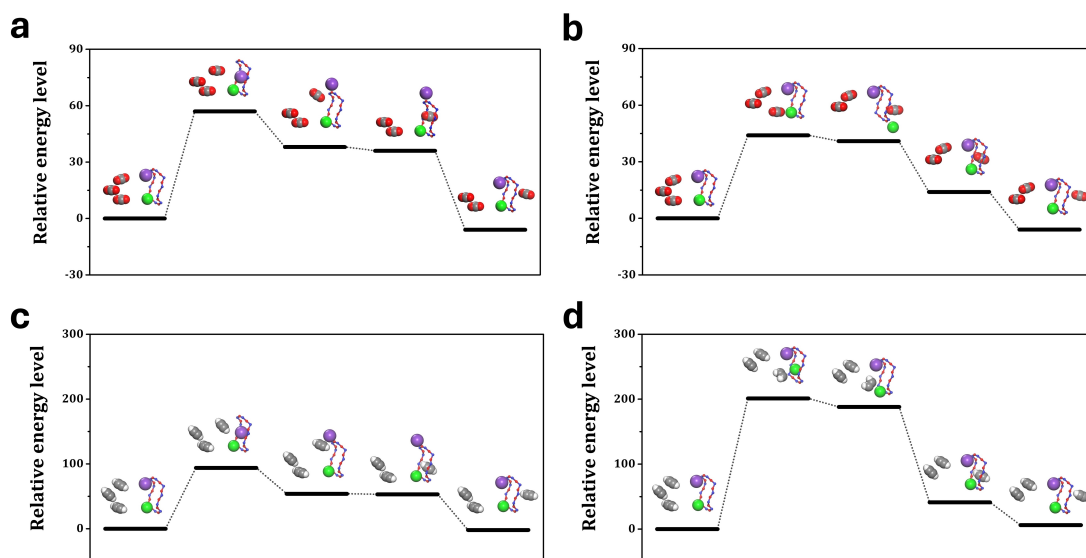

Figure 4. Illustration of the molecular trapdoor mechanism and the corresponding energy levels calculated by DFT. (**a**) The interaction between CO_2 and K^+ when passing through 10MR-K/Sr. (**b**) The interaction between CO_2 and Sr^{2+} when passing through 10MR-K/Sr. (**c**) The interaction between C_2H_2 and K^+ when passing through 10MR-K/Sr. (**d**) The interaction between C_2H_2 and Sr^{2+} when passing through 10MR-K/Sr.

an energy barrier of 41 kJ/mol). Notably, Sr^{2+} exhibits a transient affinity towards CO_2 during the homing process, underscoring the intricate host-guest dynamics (Figure 4b). According to the simulation results, CO_2 can pass through the door of 10MRs settled by Sr^{2+}-K^+ pairs with a low energy barrier of 44 kJ/mol (preferential interaction with Sr^{2+}). Interestingly, CO_2 can easily pass through the door of 10MRs settled by double Sr^{2+} cations (10MR-Sr/Sr) with exactly the same energy barrier of 44 kJ/mol (Supporting Information, Figure S28). That is, CO_2 molecules can diffuse into the internal cavities of HEU zeolite for adsorption by passing through the door of 10MRs, driven by the robust interaction between CO_2 and the dooring-keeping Sr^{2+} cation.

Upon the proximity of C_2H_2 to the 10MR-K/Sr, the interplay between C_2H_2 and K^+ was first considered with a trajectory mirroring that of CO_2, namely the migration of K^+ towards the center of the ring before veering towards the periphery. However, both the transition and migration states necessitate high energy barriers, registering at 94 kJ/mol and 54 kJ/mol, respectively (Figure 4c). Considering the interaction between C_2H_2 and Sr^{2+} in 10MR-K/Sr, the subtle relocation of Sr^{2+} towards the center of the ring and subsequent migration towards the periphery necessitate a formidable energy barrier of 201 kJ/mol and 188 kJ/mol, respectively. The approaching C_2H_2 molecules undergo structure deformation owing to the strong repulsion from the positive charge towards the positive center of the molecule (H atom), making this mission impossible (Figure 4d). Similarly, it is impossible for C_2H_2 molecules to pass through the doors of 10MR-Sr/Sr (energy barriers > 200 kJ/mol, Supporting Information, Figure S29). DFT simulation results reveal the vital role of extraframework cations on the inverse CO_2-C_2H_2 separation by constructing trapdoor for molecular recognition, namely the molecular trapdoor. Specifically, C_2H_2 molecules cannot pass through the doors of 10MRs with Sr^{2+} as the gate-keeping cations, while they might be able to diffuse into the internal cavities through the doors of 10MRs upon the transient migration of gate-keeping K^+ (even though with high energy barriers). In this context, more residual K^+ as the gate-keeping cations should correspond to higher amount of C_2H_2 molecules adsorbed by Sr/K-HEU zeolite, as confirmed by the static C_2H_2 sorption isotherms (Supporting Information, Figure S30). If Sr-HEU zeolite free of residual K^+ could be prepared, perfect CO_2/C_2H_2 selectivity can be expected in both static adsorption isotherms and dynamic breakthrough experiments. In addition, we have to clarify that it is difficult to use only simulations to treat such a complicated system. However, with the combination of experimental observations and theoretical simulations, new insight into the molecular trapdoor effect can be gained.

Conclusion

The separation of CO_2 and C_2H_2 is an essential process to produce high-quality C_2H_2 for industrial applications, which faces formidable challenges posed by the almost identical physical properties of the two molecules. We report herein the first example of zeolite adsorbent, namely Sr/K-HEU, for inverse CO_2-C_2H_2 separation utilizing the molecular trapdoor effect. Experimentally, Sr/K-HEU shows unprecedent dynamic CO_2/C_2H_2 selectivity of 48.0, sustainable dynamic CO_2 uptake of 0.96 mmol/g and perfect recyclability in CO_2-C_2H_2 separation, demonstrating its great potential for practical applications *via* a straightforward temperature-swing adsorption process.

The precise structure of Sr/K-HEU has been identified by 3D ED, showing 10MRs within channel A of HEU zeolite settled by Sr^{2+}-K^+ pairs or double Sr^{2+} as the gate–keeping cations. The interplay between the guest molecules (CO_2 or C_2H_2) and the gate–keeping cations (Sr^{2+} or K^+) has been investigated by DFT calculations. Typically, CO_2 can easily pass through the 10MRs of HEU zeolite upon the temporary and reversible deviation of gate-keeping cations while C_2H_2 cannot, thereby realizing the inverse CO_2-C_2H_2 separation through the molecular trapdoor mechanism. Overall, an example of molecular trapdoor in Sr/K-HEU zeolite is demonstrated for the inverse CO_2-C_2H_2 separation with the underlying mechanism well interpreted, providing new thoughts for separation by zeolites.

Conflict of Interest

The authors declare no conflict of interest.

Keywords: molecular trapdoor · HEU zeolite · CO_2-C_2H_2 inverse separation · extra-framework cations

[1] P. Pässler, W. Hefner, K. Buckl, H. Meinass, A. Meiswinkel, H. J. Wernicke, G. Ebersberg, R. Müller, J. Bässler, H. Behringer, *Acetylene in Ullmann's Encyclopedia of Industrial Chemistry*, Vol. 1, Weinheim: Wiley-VCH Verlag GmbH & Co. KGaA, **2012**, pp. 277–326.

[2] R. Matsuda, R. Kitaura, S. Kitagawa, Y. Kubota, R. V. Belosludov, T. C. Kobayashi, H. Sakamoto, T. Chiba, M. Takata, Y. Kawazoe, Y. Mita, *Nature* **2005**, *436*, 238.

[3] I. T. Trotuş, T. Zimmermann, F. Schüth, *Chem. Rev.* **2014**, *114*, 1761.

[4] J. R. Li, R. J. Kuppler, H. C. Zhou, *Chem. Soc. Rev.* **2009**, *38*, 1477.

[5] J. Pei, K. Shao, J. X. Wang, H. M. Wen, Y. Yang, Y. Cui, R. Krishna, B. Li, G. Qian, *Adv. Mater.* **2020**, *32*, 1908275.

[6] L. Z. Cai, Z. Z. Yao, S. J. Lin, M. S. Wang, G. C. Guo, *Angew. Chem. Int. Ed.* **2021**, *60*, 18223.

[7] L. Zhang, K. Jiang, L. Yang, L. Li, E. Hu, L. Yang, K. Shao, H. Xing, Y. Cui, Y. Yang, B. Li, B. Chen, G. Qian, *Angew. Chem. Int. Ed.* **2021**, *60*, 15995.

[8] R. B. Lin, S. Xiang, W. Zhou, B. Chen, *Chem* **2020**, *6*, 337.

[9] J. Li, P. M. Bhatt, M. Eddaoudi, Y. Liu, *Adv. Mater.* **2020**, *32*, 2002563.

[10] Z. Di, C. Liu, J. Pang, C. Chen, F. Hu, D. Yuan, M. Wu, M. Hong, *Angew. Chem. Int. Ed.* **2021**, *60*, 10828.

[11] Y. Yang, H. Zhang, Z. Yuan, J. Q. Wang, F. Xiang, L. Chen, F. Wei, S. Xiang, B. Chen, Z. Zhang, *Angew. Chem. Int. Ed.* **2022**, *61*, e202207579.

[12] Z. Niu, X. Cui, T. Pham, G. Verma, P. C. Lan, C. Shan, H. Xing, K. A. Forrest, S. Suepaul, B. Space, A. Nafady, A. M. Al-Enizi, S. Ma, *Angew. Chem. Int. Ed.* **2021**, *60*, 5283.

[13] L. Yang, L. Yan, Y. Wang, Z. Liu, J. He, Q. Fu, D. Liu, X. Gu, P. Dai, L. Li, X. Zhao, *Angew. Chem. Int. Ed.* **2021**, *60*, 4570.

[14] Q. Dong, X. Zhang, S. Liu, R. B. Lin, Y. Guo, Y. Ma, A. Yonezu, R. Krishna, G. Liu, J. Duan, R. Matsuda, W. Jin, B. Chen, *Angew. Chem. Int. Ed.* **2020**, *59*, 22756.

[15] Z. Zhang, C. Kang, S. B. Peh, D. Shi, F. Yang, Q. Liu, D. Zhao, *J. Am. Chem. Soc.* **2022**, *144*, 14992.

[16] S. Chen, N. Behera, C. Yang, Q. Dong, B. Zheng, Y. Li, Q. Tang, Z. Wang, Y. Wang, J. Duan, *Nano Res.* **2021**, *14*, 546.

[17] X. Zhang, R. B. Lin, H. Wu, Y. Huang, Y. Ye, J. Duan, W. Zhou, J. R. Li, B. Chen, *Chem. Eng. J.* **2022**, *431*, 134184.

[18] H. Xu, Y. He, Z. Zhang, S. Xiang, J. Cai, Y. Cui, Y. Yang, G. Qian, B. Chen, *J. Mater. Chem. A* **2013**, *1*, 77.

[19] Y. Belmabkhouta, Z. Zhang, K. Adila, P. M. Bhatta, A. Cadiaua, V. Solovyevaa, H. Xing, M. Eddaoudia, *Chem. Eng. J.* **2019**, *359*, 32.

[20] W. Wang, G. D. Wang, B. Zhang, X. Y. Li, L. Hou, Q. Y. Yang, B. Liu, *Small* **2023**, *19*, 2302975.

[21] Q. Liu, S. G. Cho, J. Hilliard, T.-Y. Wang, S.-C. Chien, L.-C. Lin, A. C. Co, C. R. Wade, *Angew. Chem. Int. Ed.* **2023**, *62*, e202218854.

[22] B. K. Ling, M. Zeng, T. Zhang, J. W. Cao, R. Yang, L. Cheng, C. Y. Zhang, Y. Wang, K. J. Chen, *Chem. Commun.* **2023**, *59*, 10952.

[23] C. He, P. Zhang, Y. Wang, Y. Zhang, T. Hu, L. Li, J. Li, *Sep. Purif. Technol.* **2023**, *304*, 122318.

[24] D. S. Choi, D. W. Kim, D. W. Kang, M. Kang, Y. S. Chae, C. S. Hong, *J. Mater. Chem. A* **2021**, *9*, 21424.

[25] L. Li, J. Wang, Z. Zhang, Q. Yang, Y. Yang, B. Su, Z. Bao, Q. Ren, *ACS Appl. Mater. Interfaces* **2019**, *11*, 2543.

[26] Y. Shi, Y. Xie, H. Cui, Y. Ye, H. Wu, W. Zhou, H. Arman, R. B. Lin, B. Chen, *Adv. Mater.* **2021**, *33*, 2105880.

[27] Y. Gu, J. Zheng, K. Otake, M. Shivanna, S. Sakaki, H. Yoshino, M. Ohba, S. Kawaguchi, Y. Wang, F. Li, S. Kitagawa, *Angew. Chem. Int. Ed.* **2021**, *60*, 11688.

[28] O. T. Qazvini, R. Babarao, S. G. Telfer, *Nat. Commun.* **2021**, *12*, 197.

[29] Y. Xie, H. Cui, H. Wu, R. B. Lin, W. Zhou, B. Chen, *Angew. Chem. Int. Ed.* **2021**, *60*, 9604.

[30] B. Ma, D. Li, Q. Zhu, Y. Li, W. Ueda, Z. Zhang, *Angew. Chem. Int. Ed.* **2022**, *61*, e202209121.

[31] S. Q. Yang, R. Krishna, H. Chen, L. Li, L. Zhou, Y. F. An, F. Y. Zhang, Q. Zhang, Y. H. Zhang, W. Li, T. L. Hu, X. H. Bu, *J. Am. Chem. Soc.* **2023**, *145*, 13901.

[32] Z. Zhang, S. B. Peh, R. Krishna, C. Kang, K. Chai, Y. Wang, D. Shi, D. Zhao, *Angew. Chem. Int. Ed.* **2021**, *60*, 17198.

[33] J. Cui, Z. Qiu, L. Yang, Z. Zhang, X. Cui, H. Xing, *Angew. Chem. Int. Ed.* **2022**, *61*, e202208756.

[34] R. T. Yang, *Gas Separation by Adsorption Processes*, Butterworth, Stoneham, **1987**, pp. 9–48.

[35] B. Yue, S. Liu, Y. Chai, G. Wu, N. Guan, L. Li, *J. Energy Chem.* **2022**, *71*, 288.

[36] P. J. Bereciartua, Á. Cantín, A. Corma, J. L. Jordá, M. Palomino, F. Rey, S. Valencia, E. W. Corcoran, P. Kortunov, P. I. Ravikovitch, A. Burton, C. Yoon, Y. Wang, C. Paur, J. Guzman, A. R. Bishop, G. L. Casty, *Science* **2017**, *358*, 1068.

[37] S. Liu, X. Han, Y. Chai, G. Wu, W. Li, J. Li, I. da Silva, P. Manuel, Y. Cheng, L. L. Daemen, A. J. Ramirez-Cuesta, W. Shi, N. Guan, S. Yang, L. Li, *Angew. Chem. Int. Ed.* **2021**, *60*, 6526.

[38] J. P. Zhang, X. M. Chen, *J. Am. Chem. Soc.* **2008**, *130*, 6010.

[39] D. D. Zhou, J. P. Zhang, *Acc. Chem. Res.* **2022**, *55*, 2966.

[40] Q. Gao, J. Xu, D. Cao, Z. Chang, X. H. Bu, *Angew. Chem. Int. Ed.* **2016**, *55*, 15027.

[41] C. Gu, N. Hosono, J. J. Zheng, Y. Sato, S. Kusaka, S. Sakaki, S. Kitagawa, *Science* **2019**, *363*, 387.

[42] J. Shang, G. Li, R. Singh, P. Xiao, J. Z. Liu, P. A. Webley, *J. Phys. Chem. C* **2013**, *117*, 12841.

[43] J. Shang, G. Li, Q. Gu, R. Singh, P. Xiao, J. Z. Liu, P. A. Webley, *Chem. Commun.* **2014**, *50*, 4544.

[44] J. Shang, G. Li, R. Singh, Q. Gu, K. M. Nairn, T. J. Bastow, N. Medhekar, C. M. Doherty, A. J. Hill, J. Z. Liu, P. A. Webley, *J. Am. Chem. Soc.* **2012**, *134*, 19246.

[45] J. Zhao, S. H. Mousavi, G. Xiao, A. H. Mokarizadeh, T. Moore, K. Chen, Q. Gu, R. Singh, A. Zavabeti, J. Z. Liu, P. A. Webley, G. K. Li, *J. Am. Chem. Soc.* **2021**, *143*, 15195.

[46] M. W. Ackleyt, R. T. Yang, *Ind. Eng. Chem. Res.* **1991**, *30*, 2523.

[47] G. Cruciani, *J. Phys. Chem. Solids* **2006**, *67*, 1973.

[48] I. K. Butikova, Y. F. Shepelev, Y. I. Smolin, *Crystallogr. Rep.* **1993**, *38*, 461.

[49] D. L. Bish, *Eur. J. Mineral* **1990**, *2*, 771.

[50] R. T. Yang, *Adsorbents: Fundamentals and Applications*, John Wiley & Sons, Hoboken, **2004**, pp. 173–183.

[51] G. M. Sheldrick, *Acta Cryst.* **2008**, *A64*, 112.

[52] R. M. Kakhki, S. Zirjanizadeh, M. Mohammadpoor, *J. Mater. Sci.* **2023**, *58*, 10555.

[53] D. A. Kennedy, F. H. Tezel, *Micropor. Mesopor. Mater.* **2018**, *262*, 235.

[54] D. A. Kennedy, M. Khanafer, F. H. Tezel, *Micropor. Mesopor. Mater.* **2019**, *281*, 123.

[55] X. Wang, N. Yan, M. Xie, P. Liu, P. Bai, H. Su, B. Wang, Y. Wang, L. Li, T. Cheng, P. Guo, W. Yan, J. Yu, *Chem. Sci.* **2021**, *12*, 8803.